The peculiarity of Malvidin 3-*O*-(6-*O*-*p*-coumaroyl) glucoside aggregation. Intra and intermolecular interactions.

Johan Mendoza,[a,‡] Joana Oliveira,[b,‡] Paula Araújo,[b] Nuno Basílio,[a] Natércia Teixeira,[b] Natércia F. Brás,[c] Fernando Pina,[a,*] Kumi Yoshida,[d] Victor de Freitas[b,*]

[a] LAQV, REQUIMTE, Departamento de Química, Faculdade de Ciências e Tecnologia, Universidade Nova de Lisboa, 2829-516 Caparica, Portugal. [*]fp@fct.unl.pt

[b] LAQV – REQUIMTE, Departamento de Química e Bioquímica, Faculdade de Ciências, Universidade do Porto, Rua do Campo Alegre, 687, 4169-007 Porto, Portugal. [*]vfreitas@fc.up.pt

[c] UCIBIO, REQUIMTE, Departamento de Química e Bioquímica, Faculdade de Ciências, Universidade do Porto, Rua do Campo Alegre, s/n, 4169-007 Porto, Portugal.

[d] Graduate School of Informatics, Nagoya University, Chikusa, Nagoya 464-8601, Japan.

[‡] These authors contributed equally to the paper.

ABSTRACT

The aggregation of malvidin 3-*O*-(6-*O*-*p*-coumaroyl) glucoside flavylium cation (OeninCoum) in water is reported. Intra and intermolecular interactions of OeninCoum were characterized by UV-vis absorption, ^{1}H NMR and circular dichroism (CD). Theoretical calculations were also performed to describe the intramolecular interactions. At higher temperature (>60°C) the intermolecular aggregates are disrupted but CD signal attributed to an intramolecular interaction remains.

Moreover, the kinetic and thermodynamic data for Oenin and OeninCoum at 50ºC and 25 ºC shows that the increase of temperature stabilizes the quinoidal base of this later.

Keywords: Oenin; coumaroyl derivatives; NMR; CD; intramolecular and intermolecular interactions; temperature.

1. Introduction

Malvidin 3-*O*-(6-*O*-p-coumaroyl) glucoside (OeninCoum), Scheme 1, is one of the most abundant anthocyanins in some grape varieties used to produce red wines[1] and in the respective by-products.[2] In spite of a few works regarding this compound that have clarified some aspects of its multistate of species in equilibrium in aqueous solutions,[3-5] the complete understanding of this system was not yet fully achieved. Comparing the behavior of the non-acylated anthocyanin Oenin with OeninCoum pointed out to a peculiar aggregation pattern of the last.[3, 4] This unique behavior is due to the presence of an acyl substituent (*p*-coumaroyl group) in the sugar residue of the anthocyanin. The dramatic effect in the physicochemical properties of anthocyanins possessing more complex poly-acylated sugars, in particular in the stabilization of the purple and blue colors, was previously reported.[6-8]

The apparently erratic behavior of OeninCoum was reflected in the conclusions achieved by different authors. For instance it was reported that "*Malvidin 3-O-(6-O-p-coumaroyl) glucoside did not shown colour enhancement (due to self-association) suggesting that the p-coumaroyl prevents self-association*".[4] However, evidence for flavylium cation interaction by intra and intermolecular association, using a synergistic combination of NMR and molecular dynamics simulation, was achieved by some of us.[3] On the other hand it was published that "*The presence of cinnamic acid acylation had a*

considerable impact on spectral and colour characteristics, causing a bathochromic shift of λ_{max}. Sugar substitution also played an important role, with a hypsochromic shift caused by the presence of glycosylation."[9]

The novelty of the present work regards the experimental approach used to study the aggregation behavior of OeninCoum in aqueous solution. Considering that Oenin and OeninCoum are identical except in the acylation pattern, all differences in physical chemical properties are necessary attribute to the effect of this acylation. Moreover, we were able to disrupt the intermolecular interactions increasing the temperature of the solutions, this supported by circular dichroism (CD) and NMR spectroscopy. The stopped flow UV/Vis experiments at 50ºC, where only the intra molecular interactions are observed serve to calculate the molar fractions of each species at the pseudo-equilibrum. This set of experiments could explain the peculiar aggregation behavior of the OeninCoum flavylium cation form and the effect of sugar acylation on the stabilization of the colored species along the pH scale.

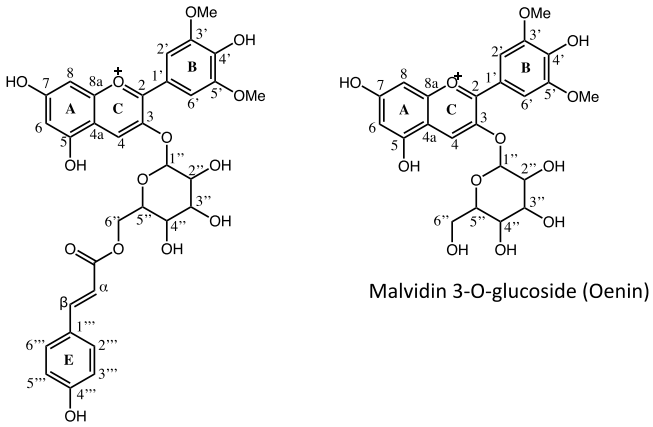

Scheme 1 – Structures of the Malvidin 3-*O*-(6-*O*-p-coumaroyl) glucoside (OeninCoum) and Malvidin 3-*O*-glucoside (Oenin) in the cation flavylium form.

2. Materials and methods.

2.1. Anthocyanins.

Oenin chloride (≥ 95%) was obtained from Extrasynthese. OeninCoum was extracted from grape pomace with an acidified (HCl) aqueous solution of methanol (50%, v/v) and purified by semi-preparative HPLC using the conditions described previously on the literature.[10]

2.2. UV-Visible and Circular Dichroism Spectroscopy.

Anthocyanins solutions ($2.5x10^{-4}$ M) were prepared using Millipore water and adjusting with HCl to 0.1 M. pH was measured on a Radiometer Copenhagen PHM240 pH/ion meter (Brønshøj, Denmark). Circular dichroism absorption and UV-Vis spectra were recorded on a Chirascan qCD spectrometer equipped with a CS/JS Recirculating Cooler (Applied Photophysics; Surrey, UK) set with a temperature ramp between 0 and 80°C under constant nitrogen flush, acquisitions were made every 5 degrees with a stabilization time of 5 min between measurements. Quartz cells (optical pathlength 1 and 0.5 cm) were used in a range of 220-700 nm with an interval of 1 nm. Two scans were averaged with baseline correction during all measurements. For the reverse pH jumps diluted stock solutions of the anthocyanins were neutralized with NaOH and Theorell and Stenhagen's buffer was used to set an specific pH, once the solutions reach the equilibrium, HCl was mixed in a stopped flow to reach pH=1 and the kinetics at 50°C were monitored on a SX20 (Applied Photophysics; Surrey, UK) spectrometer equipped with a PDA.1/UV photodiode array detector. A cut-off filter of 435 nm was used to prevent photodegradation due high the lamp intensity.

2.3. NMR.

For the ^{1}H-NMR experiments a concentration of $2.5x10^{-4}$ M of Oenin, OeninCoum and MethylCoumarate were prepared in D_2O and the pD was set to 1 by addition of DCl. ^{1}H spectra (512 scans) were recorded in a Bruker Avance III HD 600 MHz at 25, 30, 35, 40, 45, 50, 55 and 60ºC.

2.4. Computational calculations.

2.4.1. Molecular Dynamics (MD) simulations.

The initial geometries of OeninCoum and Oenin were built with the GaussView software.[11] Both compounds were parametrized using the antechamber suite[12] of the AMBER 12, which includes a geometry optimization at the HF/6-31G(d)[13, 14] level of theory using the Gaussian 09 software[11] and a RESP protocol for the determination of atomic point charges. Then, geometry optimizations and MD simulations were carried out with the AMBER 12 simulation package[15], using the Generalized Amber Force Field (GAFF)[16]. In these simulations, an explicit solvation with a 12 Å rectangular pre-equilibrated TIP3P water box was used (around OeninCoum or Oenin). Each system was equilibrated with an MD simulation of 100 ps in the NVT ensemble and using periodic boundaries conditions. This was followed by 10 ns of MD simulation in the NPT ensemble. The pressure (1 atm) and the temperature (298 K) were controlled by a Berendsen barostat and a Langevin thermostat, respectively.[17] Ten structures of OeninCoum and Oenin were extracted from the respective MD trajectories. Regarding the NMR data, the smaller H6/H8 – H4 distances deduced from NOESY spectra were used as metric to obtain the OeninCoum geometries, whilst the pairwise root mean square deviation (RMSd) between frames was used to extract the representative geometries of Oenin. These structures were used for further Quantum Mechanics (QM) energy calculations.

2.4.2. DFT calculations.

Each geometry of both molecules were optimized by employing the B3P86[18] hybrid functional and the 6-31+G(d,p)[14] basis set. This level of theory was chosen due to its accuracy to calculate thermodynamic properties for similar molecules.[19] The integral equation formalism polarizable continuum model (IEFPCM)[11] method was used to

account the water dissolution. Vibrational analysis was done at the same level of theory to confirm local minima without imaginary frequencies.

3. Results and discussion.

Upon extraction and HPLC purification followed by lyophilization, the behaviour of pure OeninCoum in water at pH 1.0 is not reproducible. Indeed, different solubility of the powder, different colors from purple to red, and also the precipitation of a bluish powder poorly soluble at higher concentrations could occur.

3.1. CD.

The circular dichroism (CD) spectra of a solution of OeninCoum is presented in **Figure 1a** and it shows two different signals in the visible region. Regarding the respective absorption spectra, **Figure 1b**, at 20°C some small particles in suspension responsible for the characteristic raise of the absorption due to light scattering are visible at naked eye up to 600 nm. The data of **Figure 1** can be interpreted by the existence of inter and intramolecular interactions in the OeninCoum solution at 20°C. As expected, heating the solution disrupts the characteristic signal of the intermolecular interactions (as observed in the Oenin CD spectra), relative to the π-π anti-clockwise molecular stacking.[20] At 70°C the signal that remains in the visible region can be interpreted as a result from intramolecular interactions. This signal could be attributed to the induced circular dichroism[21-23] in the flavylium backbone resulting from the coumaroyl moiety interaction. Moreover, **Figure 1c** shows the CD spectra of OeninCoum at 70°C in three different concentrations ($5.0x10^{-5}$ M; $1.2x10^{-4}$ M; $2.5x10^{-4}$ M) upon normalization. Curiously, the signal does not change, supporting the absence of intermolecular interactions under these conditions. It is well known that the dilution effect reduces intermolecular interactions while intramolecular one's are

much less or not affected which is a very good indication that this latter interaction could take place.

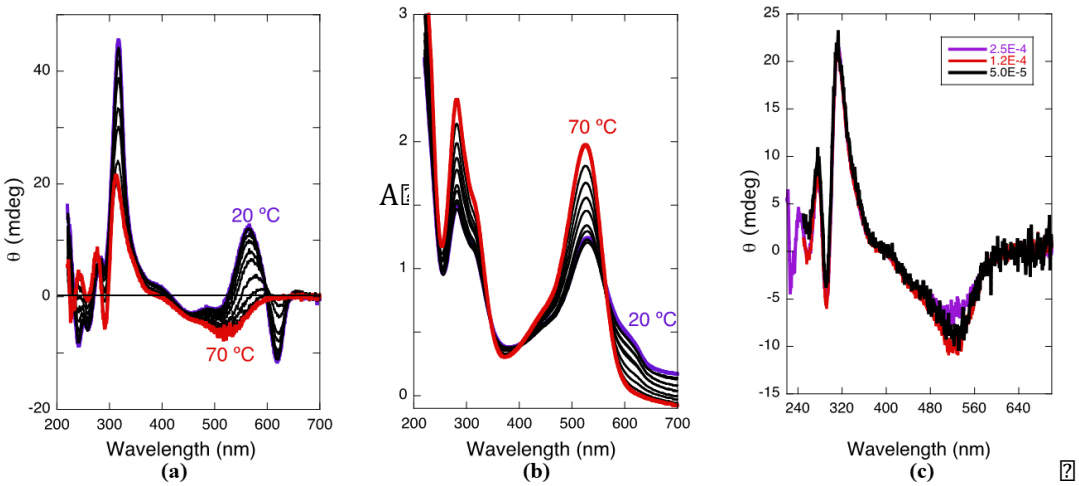

Figure 1 – (a) Circular dichroism spectra of OeninCoum, in water 2.5x10^{-4} M, pH 1.0, as a function of temperature (20–70°C); (b) Absorption spectra of the same solutions of (a); (c) CD spectra at 70°C upon normalization at three concentrations (5.0x10^{-5} M; 1.2x10^{-4} M; 2.5x10^{-4} M).

The CD spectra of anthocyanins 3-*O*-mono-glucosides including the one of Oenin were previously reported.[4, 9, 20, 24-26] Oenin lacks the coumaroyl group responsible for the intramolecular interactions in OeninCoum and therefore only intermolecular aggregation is possible for oenin.[20] In the CD spectra of Oenin (**Figure 2**) the characteristic signal of intermolecular interactions (Cotton effect) disappear with the increase of temperature but no other CD signal is observed in the visible region. Comparing the CD spectra of Oenin and OeninCoum, it is possible to observe that in this latter there is an additional signal in the visible region that remains in the spectra after heating the solution at 70°C. This is clearly observed in **Figure 2c** where the CD spectra of OeninCoum, and the one of Oenin are compared for the same concentration and pH.

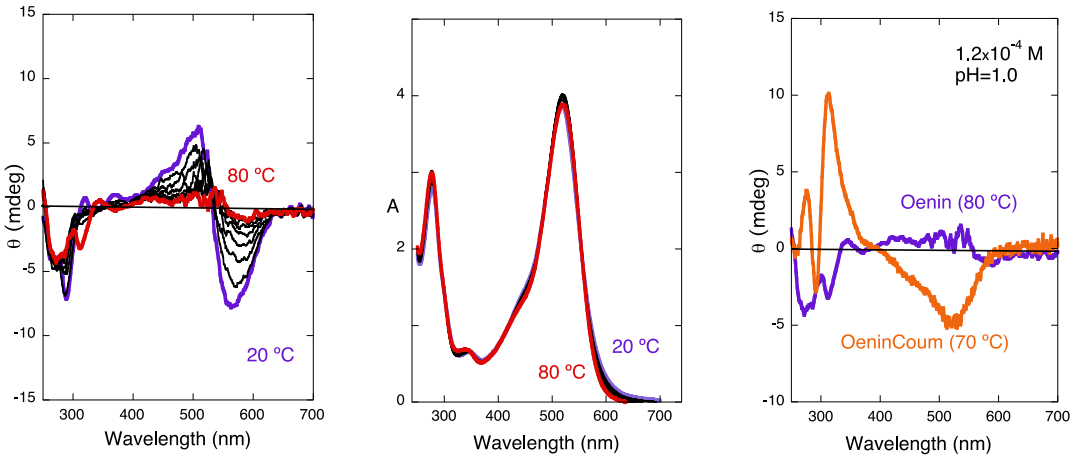

Figure 2 – (a) Circular dichroism spectra of Oenin, in water $1.2x10^{-4}$ M, pH 1.0, as a function of temperature (20–80°C); (b) Absorption spectra of (a); (c) comparison of the CD spectra of OeninCoum and Oenin in the same conditions.

3.2. NMR.

Figure 3a shows the ^{1}H NMR spectra in the aromatic region of the OeninCoum at pH 1 as function of the temperature. At 25°C, protons signals present a broad shape with small resolution which was not observed for Oenin (**Figure 3b**) and this is indicative of the presence of intermolecular interactions in OeninCoum. With the increase of the temperature up to 60°C it is observed the sharpening of all peaks and their shift to lower fields.

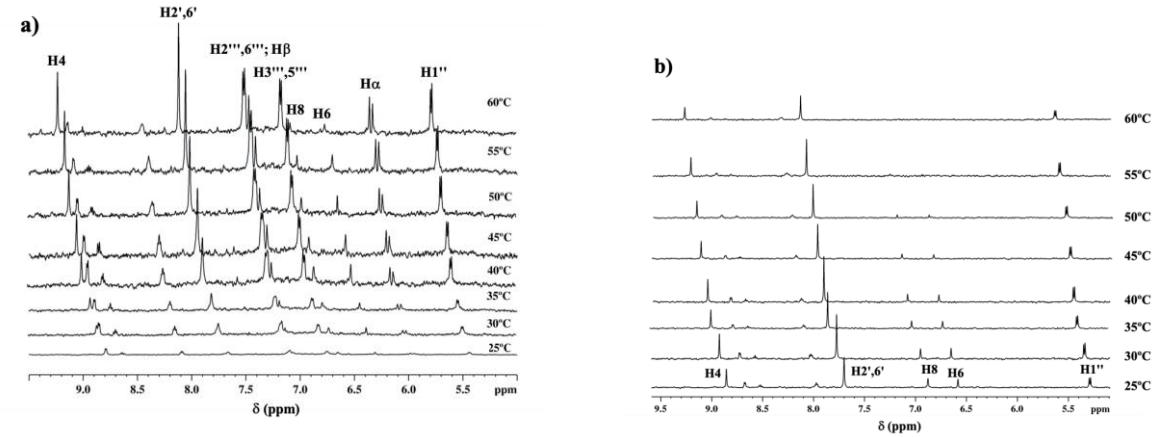

Figure 3 – ^{1}H spectra in the aromatic region of a) OeninCoum, $2.5x10^{-4}$ M and b) Oenin, $2.5x10^{-4}$ M, in D_2O at pD 1 as function of the temperature.

The difference between the chemical shifts at different temperatures of the phenylbenzopyrylium core protons in OeninCoum and Oenin is reported in **Figure 4a** and **Table S1** (ESI). Similarly, the chemical shift difference between the coumaroyl protons of OeninCoum and Methyl-*p*-*trans*-coumarate (MeCoum) is presented in **Figure 4b** and **Table S2** (ESI). At high temperature, intermolecular interactions do not exist in both compounds or are significantly reduced. Thus, it is expected that the chemical shifts difference between OeninCoum and Oenin ($\Delta\delta$: δ(ppm)OeninCoum–δ(ppm)Oenin) would converge to zero in the case of the following two hypothetical reasons: i) in the absence of any interactions of the coumaroyl moiety with the flavylium core, or, ii) if the proximity of the coumaroyl moiety had no effects on the flavylium moiety signals. **Figure 4a** shows that there are very significant differences in the Δδ of some protons but they are more or less preserved during the temperature changes. While protons H2', H6' and H4 are less affected (chemical shifts difference is around zero) those in position H6 and H8 have a negative shift and the protons of the methoxyl groups and H1" of the sugar moiety present a positive shift by the presence of the coumaroyl group. Moreover, comparing the coumaroyl moiety ^{1}H NMR signals in OeninCoum with the ones of methyl coumarate of the same concentration as those of OeninCoum (Fig. 4b, $\Delta\delta$: δ(ppm)OeninCoum–δ(ppm)Methyl-*p*-Coum), the H3"', 5"' chemical shift is similar ($\Delta\delta$ ~0), while the rest are highly affected (up field shifted). This data confirms the effect of the coumaroyl intramolecular folding over the phenylbenzopyrylium core of OeninCoum affecting both coumaroyl and phenylbenzopyrylium ^{1}H NMR signals.

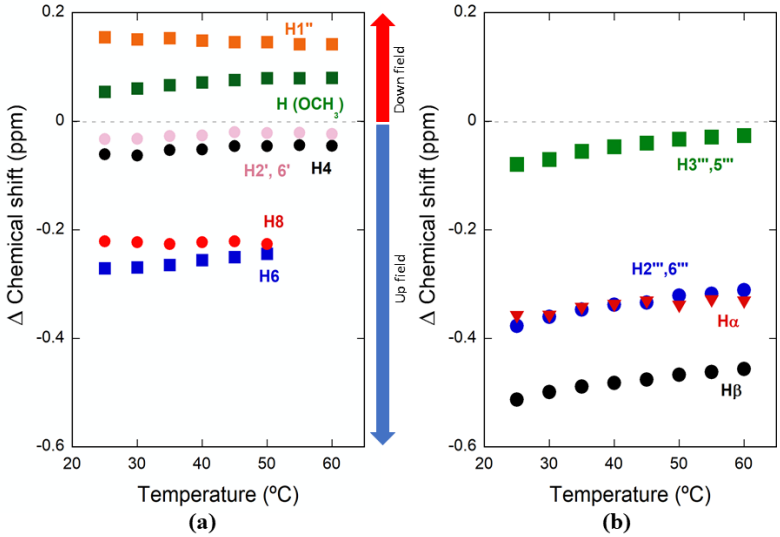

Figure 4 – Chemical shifts difference between (a) the phenylbenzopyrylium core protons of OeninCoum and Oenin and (b) the coumaroyl protons of OeninCoum and methyl-*p*-*trans*-coumarate at different temperatures.

3.3. Computational calculations.

Theoretical quantum mechanics (DFT) calculations were performed on ten different geometries of OeninCoum and Oenin extracted from the respective MD simulation. **Table S3** in ESI displays the relative energies (ΔE) of the various conformations. OeninCoum geometries can be assembled in two groups, depending of the relative position of the coumaroyl moiety: one composed by conformations 1 to 7 that have similar geometries, and other one composed by conformers 8 to 10. The main difference between the two groups is the position of the coumaroyl group. The most stable conformation of each group (conformers 1 and 8) have an energy difference of 2.6 kcal/mol). In contrast, all geometries of Oenin are quite similar, being the conformation 1 the representative one for this compound. **Figure S1** (ESI) illustrates the molecular geometries of the most stable conformers of OeninCoum (representative of each geometry group) and Oenin. The obtained structures are similar to other acylated anthocyanins reported previously.[27]

The electrostatic potential maps of both conformers of OeninCoum were also determined as well as the main electrostatic/dispersion interactions and the distances between some atoms (See **Figure S2** and **Table S4** in ESI). It was observed that the main difference between the two stable conformers is the π-stacking between the flavylium and p-coumaroyl units. According to **Figure S2**, the ground state electronic density of the p-coumaric acid moiety and the A and C rings of the flavylium backbone are overlapped (red circle) in the conformer 8. However, this particular π-stacking is absent in conformer 1. The latter agrees with the structure described in our previous self-association study.[3] Conformer 1 has a moderate interaction between H4 and the oxygen of the carbonyl group, whilst the conformer 8 of OeninCoum possesses four weak intramolecular interactions: a C=O—π interaction of the O in the carbonyl group with the C ring, a C=O—H interaction between the carbonyl group and the H1" of glucose; a C–H—π interaction between the Hα and the A ring, and a C-O—H interaction from O-2" to OMe-5' (See **Figure 5** and **Table S4**).[28]

Conformers 8 and 1 of OeninCoum and Oenin, respectively, were selected as models for further analysis. As expected, no intramolecular interactions between the flavylium moiety and the sugar unit were observed in Oenin. These interactions explain the data reported in **Figure 4** where the δ in chemical shifts is positive for H1" and protons of OMe-3',5', being these protons deshielded and their signals move downfield in the NMR spectra, as has been described for intramolecular weak hydrogen bonding.[29] In this case, two intramolecular interactions through hydrogen bonding can be observed between: i) the carbonyl present at the coumaroyl residue that acts as an acceptor and the anomeric proton of the glucose moiety H1" acting as a donor; and ii) the hydroxyl group present at carbon C2' (as acceptor) and the methoxyl groups (as donors) from the ring B.

As can be observed in **Figures 4** and **5**, the signals for H6 and H8 are shielded in OeninCoum when compared to Oenin and move up field in the NMR spectra. H3'''5''', H2'''6''', Hα and Hβ signals in the coumaroyl moiety are also shielded and the δ in chemical shifts is negative. The H3'''5''' signals are less affected because they are more distant from the flavylium core than the rest of protons in the coumaroyl moiety (**Figure 5**). The increased electronic density around these atoms observed in **Figure S2** (ESI) is due the noncovalent forces between the coumaroyl moiety and the A and C rings in the flavylium backbone.[30]

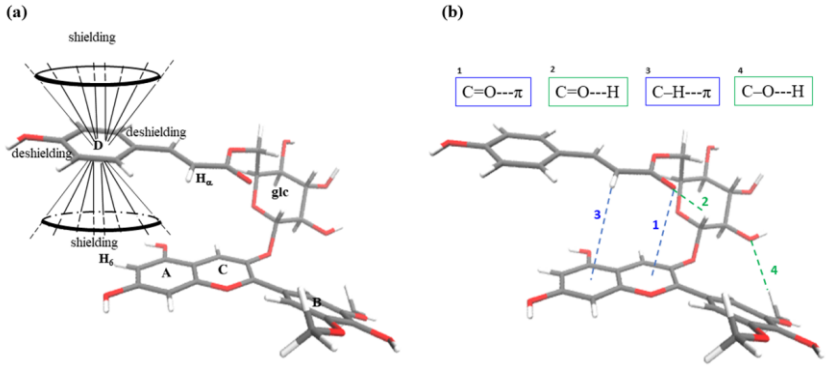

Figure 5 – OeninCoum (conformer 8) model at the B3P86/6-31^{+}G(d,p) level of theory in water representing (a) the effect of the coumaroyl moiety on the 1H NMR chemical shifts on the flavylium backbone and (b) the main electrostatic/dispersion forces between the flavylium backbone and the coumaroyl moiety.

3.4. Equilibrium network of OeninCoum species at different pHs.

Extension of this study to higher pH values is limited by the solubility of the quinoidal base. As shown in **Figure S3**, precipitation of the quinoidal base at room temperature takes place immediately after a direct pH jump to moderately acidic pHs even at low anthocyanin concentrations.

However, up 50 ºC the system is soluble allowing to carry out a series of reverse pH jumps experiments followed by stopped flow according to a methodology recently reported.[31]

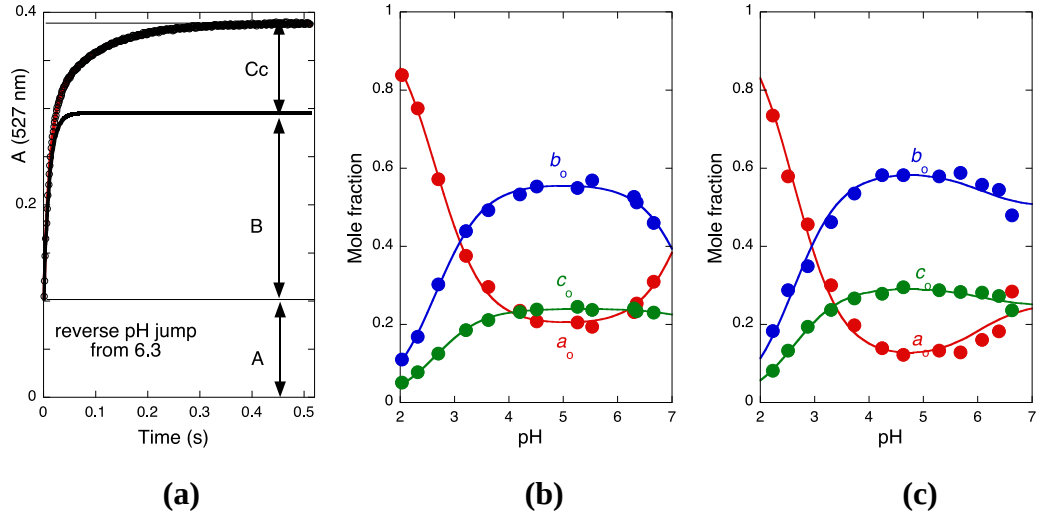

Figure 6. (a) Reverse pH jump of OeninCoum, 3.15x10^{-5} M from pH=6.3 to pH=1 at 50 ºC, followed by stopped flow; **(b)** Representation of the mole fraction distribution of the species flavylium cation plus quinoidal base and anionic quinoidal base (red), hemiketal and anionic hemiketal (blue) and cis-chalcone and anionic cis-chalcone (green) of OeninCoum, 3.15x10^{-5} M;**(c)** the same for Oenin.

Figure 6a shows the reverse pH jump of OeninCoum from pH=6.3 to pH=1 at 50 ºC. The initial absorbance is due to the conversion of quinoidal base into flavylium cation during the mixing time of the stopped flow (circa 6 ms). The faster trace is attributed to the conversion of hemiketal into flavylium cation. At this pH the hydration reaction, which is proportional to the proton concentration, becomes faster than tautomerization (change of regime). Finally, the slowest trace is due to the conversion of *cis*-chalcone in more flavylium cation via hemiketal.[32] Extension of the procedure reported in Fig. 6a to other pH values allows the calculation of the mole fraction distribution of flavylium cation plus quinoidal base (red), hemiketal (blue) and *cis*-chalcone (green), as shown in **Figure 6b** and **Figure 6c** respectively for OeninCoum and Oenin. Comparison of the

mole fraction distributions of OeninCoum and Oenin indicates that the concentration of quinoidal base is circa 2-folds higher in the former (**Figure 6**). Considering that at 50 ºC and at this concentration only the intramolecular interaction occurs, this is one more consequence of the *p*-coumaroyl residue. Table 1 summarizes the equilibrium constants calculated at 50°C and 25°C for both anthocyanins.

Table 1. Equilibrium constants of OeninCoum (50 ºC) and Oenin (50ºc and 25 ºC).

	$pK^{\wedge}_a$	$pK^{\wedge\wedge}_a$	pK_a	pK_h	K_t
OeninCoum	2.66±0.05	6.0*	3.37±0.05	2.91±0.05	0.43±0.05
Oenin (50ºC)	2.60±0.05	6*	3.56±0.05	2.85±0.05	0.50±0.05
Oenin (25ºC)	2.5±0.05	7*	3.7±0.05	2.7±0.05	0.42±0.05

*Rough estimated value. The second equilibrium is not sufficiently defined. The systems are not stable in basic medium.

In summary, the intramolecular interactions in OeninCoum can be separated from the intermolecular aggregation at high temperature and characterized by ^{1}H NMR and UV spectroscopy conjugated with circular dichroism. OeninCoum aggregates at low concentrations and forms water-insoluble aggregates. To study this molecule, it is necessary to disrupt the intermolecular interactions by increasing the temperature and at the same time the solubility of all the species in the multistate is attained. The chemical shifts of the protons in OeninCoum are significantly different from those of Oenin and methyl-*p*-coumarate, due to the intramolecular interactions.

Acknowledgements

This work was supported by the Associated Laboratory for Sustainable Chemistry, Clean Processes and Technologies LAQV. The latter is financed by national funds from UIDB/50006/2020. This work was also supported by the

project PTDC/QUI-OUT/29013/2017 funded by FCT and FEDER. J.M. is grateful for a doctoral grant from CONACYT (MEX/Ref. 288188). J.O. and N.F.B. would like to thank the FCT for their IF grants (IF/00225/2015 and IF/01355/2014). N.B. acknowledges the FCT for CEECIND/00466/2017 grant. N.T. would like to thank the contract REQUIMTE/EEC2018/PTDC/QUI-OUT/29925/2017.

References.

1. Mateus, N.; Proença, S.; Ribeiro, P.; Machado, J. M.; de Freitas, V., Grape and wine polyphenolic composition of red vitis vinifera varieties concerning vineyard altitude. *Ciencia y Tecnología Alimentaria* **2001,** *3* (2), 102-110.

2. Oliveira, J.; Alhinho da Silva, M.; Teixeira, N.; De Freitas, V.; Salas, E., Screening of Anthocyanins and Anthocyanin-Derived Pigments in Red Wine Grape Pomace Using LC-DAD/MS and MALDI-TOF Techniques. *J. Agric. Food Chem.* **2015,** *63* (35), 7636-7644.

3. Fernandes, A.; Bras, N. F.; Mateus, N.; Freitas, V. d., A study of anthocyanin self-association by NMR spectroscopy. *New Journal of Chemistry* **2015,** *39* (4), 2602-2611.

4. Lambert, S. G.; Asenstorfer, R. E.; Williamson, N. M.; Iland, P. G.; Jones, G. P., Copigmentation between malvidin-3-glucoside and some wine constituents and its importance to colour expression in red wine. *Food Chem.* **2011,** *125* (1), 106-115.

5. Moloney, M.; Robbins, R. J.; Collins, T. M.; Kondo, T.; Yoshida, K.; Dangles, O., Red cabbage anthocyanins: The influence of d-glucose acylation by hydroxycinnamic acids on their structural transformations in acidic to mildly alkaline conditions and on the resulting color. *Dyes and Pigments* **2018,** *158*, 342-352.

6. Dangles, O.; Saito, N.; Brouillard, R., Anthocyanin intramolecular copigment effect. *Phytochemistry* **1993,** *34* (1), 119-124.

7. Mendoza, J.; Basilio, N.; Pina, F.; Kondo, T.; Yoshida, K., Rationalizing the Color in Heavenly Blue Anthocyanin: A Complete Kinetic and Thermodynamic Study. *J Phys Chem B* **2018,** *122* (19), 4982-4992.

8. Trouillas, P.; Sancho-García, J. C.; De Freitas, V.; Gierschner, J.; Otyepka, M.; Dangles, O., Stabilizing and modulating color by copigmentation: insights from theory and experiment. *Chem. Rev.* **2016,** *116* (9), 4937-4982.

9. Hoshino, T.; Matsumoto, U.; Goto, T., Evidences of the self-association of anthocyanins I. Circular Dichroism of cyanin anhydrobase. *Tetrahedron Lett.* **1980,** *21* (18), 1751-1754.

10. Oliveira, J.; Fernandes, V.; Miranda, C.; Santos-Buelga, C.; Silva, A.; de Freitas, V.; Mateus, N., Color properties of four cyanidin-pyruvic acid adducts. *J. Agric. Food Chem.* **2006,** *54* (18), 6894-6903.

11. Frisch, M. J.; Trucks, G. W.; Schlegel, H. B.; Scuseria, G. E.; Robb, M. A.; Cheeseman, J. R.; Scalmani, G.; Barone, V.; Mennucci, B.; Petersson, G. A.; Nakatsuji, H.; Caricato, M.; Li, X.; Hratchian, H. P.; Izmaylov, A. F.; Bloino, J.; Zheng, G.; Sonnenberg, J. L.; Hada, M.; Ehara, M.; Toyota, K.; Fukuda, R.; Hasegawa, J.; Ishida, M.; Nakajima, T.; Honda, Y.; Kitao, O.; Nakai, H.; Vreven, T.; Montgomery Jr., J. A.; Peralta, J. E.; Ogliaro, F.; Bearpark, M. J.; Heyd, J.; Brothers, E. N.; Kudin, K. N.; Staroverov, V. N.; Kobayashi, R.; Normand, J.; Raghavachari, K.; Rendell, A. P.; Burant, J. C.; Iyengar, S. S.; Tomasi, J.; Cossi, M.; Rega, N.; Millam, N. J.; Klene, M.; Knox, J. E.; Cross, J. B.; Bakken, V.; Adamo, C.; Jaramillo, J.; Gomperts, R.; Stratmann, R. E.; Yazyev, O.; Austin, A. J.; Cammi, R.; Pomelli, C.; Ochterski, J. W.; Martin, R. L.; Morokuma, K.; Zakrzewski, V. G.;

Voth, G. A.; Salvador, P.; Dannenberg, J. J.; Dapprich, S.; Daniels, A. D.; Farkas, Ö.; Foresman, J. B.; Ortiz, J. V.; Cioslowski, J.; Fox, D. J. *Gaussian 09*, Gaussian, Inc.: Wallingford, CT, USA, 2009.

12. Wang, J.; Wang, W.; Kollman, P. A.; Case, D. A., Automatic atom type and bond type perception in molecular mechanical calculations. *J Mol Graph Model* **2006,** *25* (2), 247-60.

13. Roothaan, C. C. J., New Developments in Molecular Orbital Theory. *Reviews of Modern Physics* **1951,** *23* (2), 69-89.

14. Petersson, G. A.; Al-Laham, M. A., A complete basis set model chemistry. II. Open-shell systems and the total energies of the first-row atoms. *The Journal of Chemical Physics* **1991,** *94* (9), 6081-6090.

15. Case, D.; Darden, T.; Cheatham, I.; Duke, R. E.; Luo, R.; Crowley, M.; Walker, R. C.; Zhang, W.; Merz, K. M.; Wang, B.; Hayik, S.; Roitberg, A.; Seabra, G.; Kolossv ry, I.; Wong, K. F.; Aesani, F.; Anicek, J.; Wu; Brozell, S. R.; Steinbrecher, T.; Gohlke, H.; Yang, L.; Tan, C.; Mongan, J.; Hornak, V.; Cui, G.; Mathews, D. H.; Seetin, M. G.; Sagui, C.; Babin, V.; Kollman, P. A., **2008**.

16. Wang, J.; Wolf, R. M.; Caldwell, J. W.; Kollman, P. A.; Case, D. A., Development and testing of a general amber force field. *J Comput Chem* **2004,** *25* (9), 1157-74.

17. Izaguirre, J. A.; Catarello, D. P.; Wozniak, J. M.; Skeel, R. D., *J. Chem. Phys.* **2001,** *114*, 2090-2098.

18. Bahmann, H.; Rodenberg, A.; Arbuznikov, A. V.; Kaupp, M., A thermochemically competitive local hybrid functional without gradient corrections. *The Journal of Chemical Physics* **2007,** *126* (1), 011103.

19. Trouillas, P.; Di Meo, F.; Gierschner, J.; Linares, M.; Sancho-García, J. C.; Otyepka, M., Optical properties of wine pigments: theoretical guidelines with new methodological perspectives. *Tetrahedron* **2015,** *71* (20), 3079-3088.

20. Gavara, R.; Petrov, V.; Quintas, A.; Pina, F., Circular dichroism of anthocyanidin 3-glucoside self-aggregates. *Phytochemistry* **2013,** *88*, 92-8.

21. Allenmark, S., Induced circular dichroism by chiral molecular interaction. *Chirality* **2003,** *15* (5), 409-422.

22. Gawroński, J.; Grajewski, J., The Significance of Induced Circular Dichroism. *Organic Letters* **2003,** *5* (18), 3301-3303.

23. Mason, S. F., Induced circular dichroism. *Chemical Physics Letters* **1975,** *32* (2), 201-203.

24. Hoshino, T.; Goto, T., Effects of pH and concentration on the self-association of malvin quinonoidal base — electronic and circular dichroic studies. *Tetrahedron Lett.* **1990,** *31* (11), 1593-1596.

25. Tsutomu, H., Self-association of flavylium cations of anthocyanidin 3,5-diglucosides studied by circular dichroism and 1H NMR. *Phytochemistry* **1992,** *31* (2), 647-653.

26. Hoshino, T.; Matsumoto, U.; Goto, T., Self-association of some anthocyanins in neutral aqueous solution. *Phytochemistry* **1981,** *20* (8), 1971-1976.

27. He, J.; Li, X.; Silva, G. T. M.; Quina, F. H.; Aquino, A. J. A., Quantum Chemical Investigation of the Intramolecular Copigmentation Complex of an Acylated Anthocyanin. . *J. Braz. Chem. Soc.* **2019,** *30*, 492-498.

28. Jeffrey, G. A.; Jeffrey, G. A., *An introduction to hydrogen bonding.* . Oxford university press: New York, 1997; Vol. 32.

29. Afonin, A. V.; Ushakov, I. A.; Vashchenko, A. V.; Simonenko, D. E.; Ivanov, A. V.; Vasil'tsov, A. M.; I., M. A.; Trofimov, B. A., *Magn. Reson. Chem.* **2009,** *47*, 105-112.

30. Yoshida, K.; Kondo, T.; Goto, T., Intramolecular stacking conformation of gentiodelphin, a diacylated anthocyanin from Gentiana makinoi. *Tetrahedron* **1992,** *48* (21), 4313-4326.

31. Mendoza, J.; Basílio, N.; de Freitas, V.; Pina, F., New Procedure To Calculate All Equilibrium Constants in Flavylium Compounds: Application to the Copigmentation of Anthocyanins. *ACS Omega* **2019,** *4* (7), 12058-12070.

32. McClelland, R. A.; Gedge, S., Hydration of the flavylium ion. *J. Am. Chem. Soc.* **1980,** *102*, 5838.